Searching for redshifted 2.2 MeV neutron-capture lines from accreting neutron stars: theoretical X-ray luminosity requirements and INTEGRAL/SPI observations

Lorenzo Ducci[1], Andrea Santangelo[1], Sergey Tsygankov[2], Alexander Mushtukov[3], Carlo Ferrigno[4]

[1]Institut für Astronomie & Astrophysik, Tübingen
[2]Department of Physics and Astronomy, University of Turku
[3] Astrophysics, Department of Physics, University of Oxford
[4] ISDC Data Center for Astrophysics, Versoix

23 October 2024

EBERHARD KARLS UNIVERSITÄT TÜBINGEN

Searching for redshifted 2.2 MeV neutron-capture lines from accreting neutron stars: theoretical X-ray luminosity requirements and INTEGRAL/SPI observations

SPOILER ALERT

only upper limits

Lorenzo Ducci[1], Andrea Santangelo[1], Sergey Tsygankov[2], Alexander Mushtukov[3], Carlo Ferrigno[4]

[1] Institut für Astronomie & Astrophysik, Tübingen
[2] Department of Physics and Astronomy, University of Turku
[3] Astrophysics, Department of Physics, University of Oxford
[4] ISDC Data Center for Astrophysics, Versoix

23 October 2024

EBERHARD KARLS UNIVERSITÄT TÜBINGEN

- Kinetic energy of matter falling onto a NS is ~ 100 MeV/nucl.: ions can produce nuclear reactions; $\gamma - rays$ are emitted by the star. (Schwartzman 1970).
- Neutron capture by a proton, $n(p, \gamma)D$, with $\gamma = 2.223$ MeV, is observable in accreting NSs (Reina, Treves, Tarenghi 1974; Brecher & Burrows 1980; Bildsten et al. 1992, 1993).

- Kinetic energy of matter falling onto a NS is ~ 100 MeV/nucl.: ions can produce nuclear reactions; $\gamma - rays$ are emitted by the star. (Schwartzman 1970).
- Neutron capture by a proton, $n(p, \gamma)D$, with $\gamma = 2.223$ MeV, is observable in accreting NSs (Reina, Treves, Tarenghi 1974; Brecher & Burrows 1980; Bildsten et al. 1992, 1993).

Path to γ−ray production

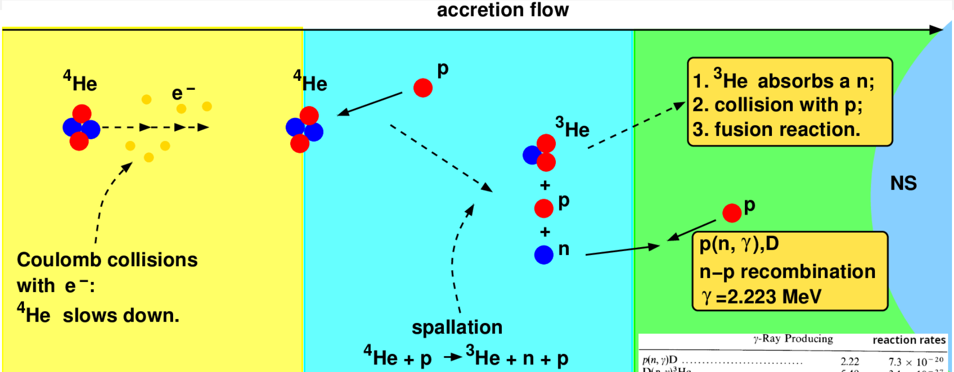

INCIDENT HELIUM DESTRUCTION CHANNELS

SPALLATION REACTION	FRAGMENT TYPE[a] p	n	D	^{3}H	^{3}He
(1) $^4\mathrm{He} + p \to p + n + {}^3\mathrm{He}$	...	0.40	...	...	0.82
(1a) $^3\mathrm{He} + p \to p + p + \mathrm{D}$	0.06	...	0.15	...	...
(1b) $^3\mathrm{He} + p \to p + 2p + n$	0.06	0.02	...	...	...
(2) $^4\mathrm{He} + p \to p + p + {}^3\mathrm{H}$	0.28	...	...	1.00	...
(2a) $^3\mathrm{H} + p \to p + p + 2n$	0.12	0.07	...	...	...
(2b) $^3\mathrm{H} + p \to n + {}^3\mathrm{He}$	−0.20	0.07	...	...	0.07
(2c) $^3\mathrm{H} + p \to \mathrm{D} + \mathrm{D}$	−0.20	...	0.05	...	...
(2d) $^3\mathrm{H} + p \to p + n + \mathrm{D}$	...	0.07	0.05	...	...
(3) $^4\mathrm{He} + p \to \mathrm{D} + {}^3\mathrm{He}$	−0.60	...	0.15	...	0.11
(4) $^4\mathrm{He} + p \to p + p + n + \mathrm{D}$	0.24	0.19	0.30	...	...
(4a) $\mathrm{D} + p \to p + p + n$	0.12	0.09	...	...	...
(5) $^4\mathrm{He} + p \to p + \mathrm{D} + \mathrm{D}$	...	...	0.30	...	...
(5a) $\mathrm{D} + p \to p + p + n$	0.12	0.09	...	...	...

[a] The entries are the fractional contribution from each reaction to the production of a particular species. These fractions were determined at an infall energy of 200 MeV nucleon^{-1}.

	γ-Ray Producing	reaction rates
$p(n,\gamma)\mathrm{D}$	2.22	7.3×10^{-20}
$\mathrm{D}(p,\gamma)^3\mathrm{He}$	5.49	3.1×10^{-27}
$^3\mathrm{H}(p,\gamma)^4\mathrm{He}$	19.81	1.4×10^{-26}

[a] Reaction rates at $T = 10^7$ K in units cm^3 s^{-1}.

Path to $\gamma-$ray production

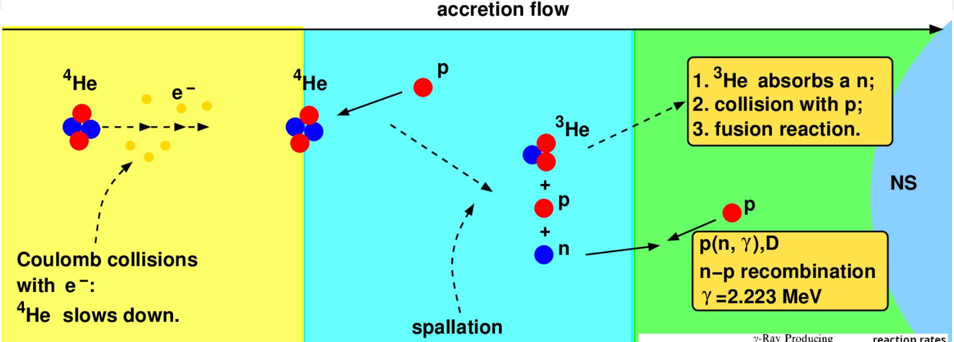

^{4}He + p → ^{3}He + n + p

INCIDENT HELIUM DESTRUCTION CHANNELS

Spallation Reaction	Fragment Type[a] p	n	D	^{3}H	^{3}He
(1) $^4\mathrm{He} + p \to p + n + {}^3\mathrm{He}$	...	0.40	...	...	0.82
(1a) $^3\mathrm{He} + p \to p + p + \mathrm{D}$	0.06	...	0.15	...	...
(1b) $^3\mathrm{He} + p \to p + 2p + n$	0.06	0.02	...	...	...
(2) $^4\mathrm{He} + p \to p + p + {}^3\mathrm{H}$	0.28	...	...	1.00	...
(2a) $^3\mathrm{H} + p \to p + p + 2n$	0.12	0.07	...	...	...
(2b) $^3\mathrm{H} + p \to n + {}^3\mathrm{He}$	−0.20	0.07	...	...	0.07
(2c) $^3\mathrm{H} + p \to \mathrm{D} + \mathrm{D}$	−0.20	...	0.05	...	...
(2d) $^3\mathrm{H} + p \to p + n + \mathrm{D}$	...	0.07	0.05	...	...
(3) $^4\mathrm{He} + p \to \mathrm{D} + {}^3\mathrm{He}$	−0.60	...	0.15	...	0.11
(4) $^4\mathrm{He} + p \to p + p + n + \mathrm{D}$	0.24	0.19	0.30	...	...
(4a) $\mathrm{D} + p \to p + p + n$	0.12	0.09	...	...	...
(5) $^4\mathrm{He} + p \to p + \mathrm{D} + \mathrm{D}$	...	...	0.30	...	...
(5a) $\mathrm{D} + p \to p + p + n$	0.12	0.09	...	...	...

[a] The entries are the fractional contribution from each reaction to the production of a particular species. These fractions were determined at an infall energy of 200 MeV nucleon^{-1}.

γ-Ray Producing		reaction rates
$p(n, \gamma)\mathrm{D}$	2.22	7.3×10^{-20}
$\mathrm{D}(p, \gamma)^3\mathrm{He}$	5.49	3.1×10^{-27}
$^3\mathrm{H}(p, \gamma)^4\mathrm{He}$	19.81	1.4×10^{-26}

[a] Reaction rates at $T = 10^7$ K in units cm^3 s^{-1}.

Detailed 2.2 MeV production mechanism in accreting NS:

- Bildsten, Salpeter, Wasserman, 1992, 1993 (ApJ 384 and 408);
- Reina, Treves, Tarenghi 1974 (A&A 32, 317)

Gravitational redshift

• Photons emitted with an intrinsic energy E_0 in the atmosphere of a NS of radius R and mass M experience a gravitational redshift to E.

• Gravitational redshift E/E_0 gives directly the stellar compactness:

$$\frac{R_{\rm NS}}{M_{\rm NS}} = \frac{2G}{[1-(E/E_0)^2]c^2}$$

$\Rightarrow$ independent method to constrain the EoS.

Line intensity

- number of 2.2 MeV photons escaping the NS atmosphere per one atom of accreted helium

- Y: mass fraction of ^4He in the accretion flow

$$F_{\mathrm{n,2.2MeV}} = Q \cdot \frac{Y}{4} \cdot \frac{1}{E_{\mathrm{i}}} \cdot F_{\mathrm{x}}$$

- X-ray flux ($F_{\mathrm{x}} \approx \dot{N}_{\mathrm{b}} E_{\mathrm{i}} / 4\pi d^2$)

- $E_{\mathrm{i}} = GMm_{\mathrm{p}}/R \approx 0.22 m_{\mathrm{p}} c^2$: kinetic energy of a baryon entering the NS atmosphere

$$F_{\mathrm{n,\,2.2MeV}} \sim 1.2 \times 10^{-6} \mathrm{ph\ cm^{-2} s^{-1}} \left(\frac{Q}{10^{-2}}\right) \left(\frac{Y}{0.25}\right) \left(\frac{162\mathrm{MeV}}{E_{\mathrm{i}}}\right) \times \left(\frac{F_{\mathrm{X}}}{3 \times 10^{-7} \mathrm{erg\ cm^{-2} s^{-1}}}\right) .$$

(Bildsten et al. 1993)

Observations:

Sco X-1: upper-limit: 2.5×10^{-5} ph cm^{-2} s^{-1} (COMPTEL; McConnell+1997)

Line intensity

- number of 2.2 MeV photons escaping the NS atmosphere per one atom of accreted helium

- Y: mass fraction of ^4He in the accretion flow

$$F_{\mathrm{n,2.2MeV}} = \boxed{Q} \cdot \boxed{\frac{Y}{4}} \cdot \boxed{\frac{1}{E_{\mathrm{i}}}} \cdot \boxed{F_{\mathrm{x}}}$$

- X-ray flux ($F_{\mathrm{x}} \approx \dot{N}_{\mathrm{b}} E_{\mathrm{i}}/4\pi d^2$)

- $E_{\mathrm{i}} = GMm_{\mathrm{p}}/R \approx 0.22 m_{\mathrm{p}} c^2$: kinetic energy of a baryon entering the NS atmosphere

$$F_{\mathrm{n,\,2.2MeV}} \sim 1.2 \times 10^{-6} \mathrm{ph\ cm^{-2} s^{-1}} \left(\frac{Q}{10^{-2}}\right) \left(\frac{Y}{0.25}\right) \left(\frac{162\mathrm{MeV}}{E_{\mathrm{i}}}\right) \times \left(\frac{F_{\mathrm{X}}}{3 \times 10^{-7} \mathrm{erg\ cm^{-2} s^{-1}}}\right) .$$

(Bildsten et al. 1993)

Observations:

Sco X-1: upper-limit: 2.5×10^{-5} ph cm^{-2} s^{-1} (COMPTEL; McConnell+1997)

Relativistic effects on emission lines of NSs

Line profiles from rotating NS are affected by:

1. *Doppler boosts*;
2. *Gravitational lensing*;
3. *frame dragging*;
4. *Stellar oblateness*.

Özel & Psaltis 2003

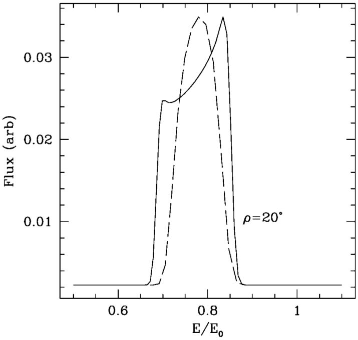

Slow rotators are best suited for searching the 2.2 MeV line (Boggs & Smith 2006; Çaliskan et al. 2009).

Relativistic effects on emission lines of NSs

Line profiles from rotating NS are affected by:

1. *Doppler boosts*;
2. *Gravitational lensing*;
3. *frame dragging*;
4. *Stellar oblateness*.

Özel & Psaltis 2003

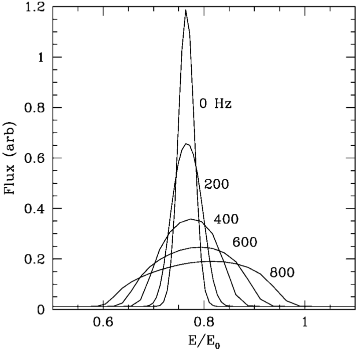

Slow rotators are best suited for searching the 2.2 MeV line (Boggs & Smith 2006; Çaliskan et al. 2009).

Optimal L_x of an XRP for the emission of 2.2 MeV photons

- Efficiency of 2.2 MeV photon production per one ^{4}He accreted, decreases as E_i becomes smaller;
- $Q \approx 0.04 \exp(-300/E_{\mathrm{i,MeV}}^{1.1})$ (Ducci+2024)
- at high $\dot{M}_\mathrm{acc}$, radiative force decelerates the accretion flow: E_kin is reduced;
- at $L_\mathrm{crit} \approx 10^{37}$ erg/s ($B \approx 10^{12}$ G), the flow is completely decelerated ($E_\mathrm{kin} = 0$);
- at $L_\mathrm{x} < L_\mathrm{crit}$: $v \approx v_\mathrm{ff}\sqrt{1 - \frac{L_\mathrm{x}}{L_\mathrm{crit}}}$

Optimal L_x of an XRP for the emission of 2.2 MeV photons

- Efficiency of 2.2 MeV photon production per one ^{4}He accreted, decreases as E_i becomes smaller;
- $Q \approx 0.04 \exp(-300/E_{\mathrm{i,MeV}}^{1.1})$ (Ducci+2024)
- at high $\dot{M}_\mathrm{acc}$, radiative force decelerates the accretion flow: E_kin is reduced;
- at $L_\mathrm{crit} \approx 10^{37}$ erg/s ($B \approx 10^{12}$ G), the flow is completely decelerated ($E_\mathrm{kin} = 0$);
- at $L_\mathrm{x} < L_\mathrm{crit}$: $v \approx v_\mathrm{ff}\sqrt{1 - \dfrac{L_\mathrm{x}}{L_\mathrm{crit}}}$

Optimal L_x of an XRP for the emission of 2.2 MeV photons

- Efficiency of 2.2 MeV photon production per one ^{4}He accreted, decreases as E_i becomes smaller;
- $Q \approx 0.04\,\exp(-300/E_{\mathrm{i,MeV}}^{1.1})$ (Ducci+2024)
- at high $\dot{M}_\mathrm{acc}$, radiative force decelerates the accretion flow: E_kin is reduced;
- at $L_\mathrm{crit} \approx 10^{37}$ erg/s ($B \approx 10^{12}$ G), the flow is completely decelerated ($E_\mathrm{kin} = 0$);
- at $L_\mathrm{x} < L_\mathrm{crit}$: $v \approx v_\mathrm{ff}\sqrt{1 - \dfrac{L_\mathrm{x}}{L_\mathrm{crit}}}$
- $$\xcancel{F_{\mathrm{n,\,2.2MeV}} \approx 1.2 \times 10^{-6}\mathrm{ph\ cm^{-2}s^{-1}} \left(\frac{Q}{10^{-2}}\right)\left(\frac{Y}{0.25}\right)\left(\frac{162\mathrm{MeV}}{E_\mathrm{i}}\right) \times \left(\frac{F_\mathrm{X}}{3 \times 10^{-7}\mathrm{erg\ cm^{-2}s^{-1}}}\right).}$$

Optimal L_x of an XRP for the emission of 2.2 MeV photons

- Efficiency of 2.2 MeV photon production per one ^{4}He accreted, decreases as E_i becomes smaller;
- $Q \approx 0.04 \exp(-300/E_{\mathrm{i,MeV}}^{1.1})$ (Ducci+2024)
- at high $\dot{M}_\mathrm{acc}$, radiative force decelerates the accretion flow: E_kin is reduced;
- at $L_\mathrm{crit} \approx 10^{37}$ erg/s ($B \approx 10^{12}$ G), the flow is completely decelerated ($E_\mathrm{kin} = 0$);
- at $L_\mathrm{x} < L_\mathrm{crit}$: $v \approx v_\mathrm{ff}\sqrt{1 - \dfrac{L_\mathrm{x}}{L_\mathrm{crit}}}$
- $$\xcancel{F_{\mathrm{n,\,2.2MeV}} \sim 1.2 \times 10^{-6}\,\mathrm{ph\ cm^{-2}s^{-1}} \left(\frac{Q}{10^{-2}}\right)\left(\frac{Y}{0.25}\right)\left(\frac{162\,\mathrm{MeV}}{E_\mathrm{i}}\right) \times \left(\frac{F_\mathrm{X}}{3 \times 10^{-7}\,\mathrm{erg\ cm^{-2}s^{-1}}}\right).}$$

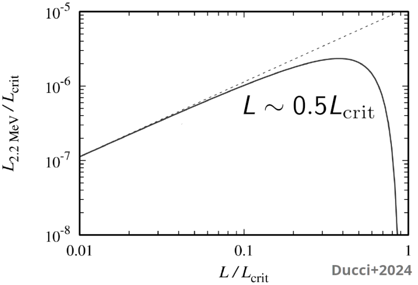

Fig. 1. Expected luminosity of the 2.2 MeV line, $L_{2.2\,\mathrm{MeV}}$, as a function of the total accretion luminosity L of an XRP. Both axes are scaled by the critical accretion luminosity L_crit. At low mass accretion rates and luminosity, the flux in the 2.2 MeV line is proportional to the total accretion luminosity. At high mass accretion rates, however, the radiative force decelerates the accretion flow above the NS surface, which results in a sharp drop in luminosity in the 2.2 MeV line.

SPI upper-limits vs expectations

Source name	net exposure	L_x	3σ u.l. 2.2 MeV line				
	(ks)	(erg s^{-1})	10^{-4}ph cm^{-2} s^{-1}				
			FWHM: (keV)	10	20	40	100
A 0535+26	1631	3×10^{36}		7.5	9.5	11	16
GX 304−1	381	3×10^{36}		18	15	22	36
Vela X-1	5345	3×10^{36}		2.4	3.0	3.8	7.2
X Persei	3050	6×10^{34}		4.4	5.2	8.2	9.8
Sco X-1	4495	$\sim 10^{38}$		2.8	3.6	5.3	9.6

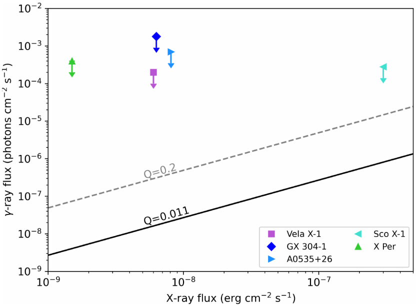

data analysed with: SPIDAI: https://sigma2.irap.omp.eu/integral/spidai

'MeV gap' and future MeV missions

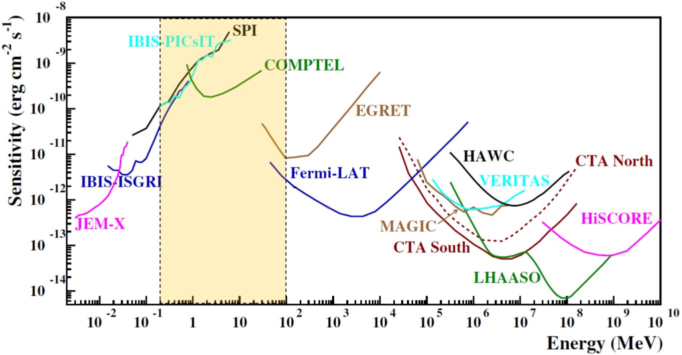

- COSI ($\sim$ 2027; see talk by Julien Malzac on Thursday);
- COSI will achieve a 3σ line point source sensitivity of $2 \times 10^{-6}\,\mathrm{ph\,cm^{-2}\,s^{-1}}$ in 1 Ms;
- concept missions: e-ASTROGAM, MASS, MeVGRO, ...

Flux concentrating telescopes

- Smaller detector sizes $\rightarrow$ lower instrumental background;
- a viable option: γ-ray optics that employ the Laue lenses: Bragg diffraction from arrays of crystals (e.g., Virgilli+2022a);
- mission concepts *ASTENA* (Virgilli+2022b); *FIONA* (IHEP)

$$E \propto \frac{F}{dr}$$

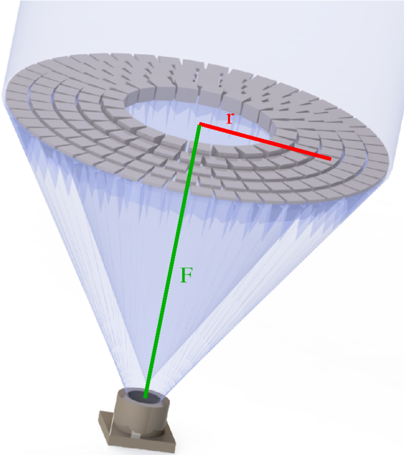

where:

- F: focal length;
- r: crystal distance from axis;
- d: spacing of the crystal lattice planes.

Drawbacks:

- Technological challenges (production of crystals, mounting, alignment, ...);
- strongly energy dependent: high sensitivity on a limited pass-band.

$\hookrightarrow$ *possible solution:* tunable Laue lens (Lund 2021): change F and orientation of the crystals.